THE JOURNAL OF PHYSICAL CHEMISTRY A

Article

Gas Phase Thermometry via Multi-Time-to-Frequency Mapping of Coherence Dephasing

Orin Yue, Marshall Bremer, Dmitry Pestov, James R. Gord, Sukesh Roy, and Marcos Dantus

J. Phys. Chem. A, **Just Accepted Manuscript** • DOI: 10.1021/jp3010103 • Publication Date (Web): 29 Jun 2012

Gas-Phase Thermometry via Multi-Time-to-Frequency Mapping of Coherence Dephasing

Orin Yue,[1,] Marshall T. Bremer,[1] Dmitry Pestov,[2] James R. Gord,[3] Sukesh Roy,[4] and Marcos Dantus[1,2]*

[1]Department of Chemistry, Michigan State University, East Lansing MI 48823, USA

[2]Biophotonic Solutions Inc., 1401 East Lansing Drive, Suite 112, East Lansing, MI 48823, USA

[3]Air Force Research Laboratory, Propulsion Directorate, Wright-Patterson AFB, OH 45433, USA

[4]Spectral Energies LLC, 5100 Springfield Street, Suite 301, Dayton, OH 45431, USA

[*]E-mail: dantus@chemistry.msu.edu

We demonstrate a single-beam coherent anti-Stokes Raman scattering (CARS) technique for gas-phase thermometry that assesses the species-specific local gas temperature by single-shot time-to-frequency mapping of Raman-coherence dephasing. The proof-of-principle experiments are performed with air in a temperature-controlled gas cell. Impulsive excitation of molecular vibrations by an ultrashort pump/Stokes pulse is followed by multi-pulse probing of the 2330-cm^{-1} Raman transition of N_2. This sequence of colored probe pulses, delayed in time with respect to each other and corresponding to three isolated spectral bands, imprints the coherence dephasing onto the measured CARS spectrum. For calibration purposes, the dephasing rates are recorded at various gas temperatures, and the relation is fitted to a linear regression. The calibration data are then used to determine the gas temperature and are shown to provide better than 15 K accuracy. The described approach is insensitive to pulse energy fluctuations and can, in principle, gauge the temperature of multiple chemical species in a single laser

shot, which is deemed particularly valuable for temperature profiling of reacting flows in gas-turbine combustors.

KEYWORDS: femtosecond, CARS, thermometry, single-shot, multi-pulse probing, multi-color, time-resolved, frequency-resolved

Introduction

It has been over a decade since time-resolved, femtosecond coherent anti-Stokes Raman scattering (fs-CARS) spectroscopy, used at the time to explore coherent wave-packet dynamics,[1] was suggested as a tool for flame thermometry.[2,3] The coherence-dephasing time, probed directly by CARS and other four-wave mixing processes, provides a direct measurement of the local temperature for the species being probed.[4] Although frequency-resolved CARS techniques for flame thermometry are well established[5] they generally rely on obtaining high-resolution spectra; in a particular example, the signal from vibrational "hot bands," *i.e.*, higher vibrational levels populated at high gas temperatures. Therefore, frequency-resolved CARS measurements require precise modeling of the collisional broadening occurring within the time-scale of the experiment (typically, nanoseconds). On the femtosecond time scale, collisional-broadening effects can be neglected, greatly simplifying data analysis and allowing one to isolate the temperature-dependent markers such as coherence-dephasing rate.[6] Data analysis can be further simplified by the use of pulse shaping and pulse timing for separation of the instantaneous electronic response from the Raman-resonant signal. Finally, the intrinsically broad spectral bandwidth of femtosecond lasers enables impulsive excitation of high-wavenumber Raman transitions and simultaneous excitation of multiple vibrational modes by a single laser pulse.

The benefits of the femtosecond time scale have been recognized experimentally for time- and frequency-domain methods. Hybrid femtosecond/picosecond CARS, which sacrifices the spectral resolution of nanosecond CARS for pulse timing and picosecond probing, has been demonstrated to provide some important advantages over conventional frequency-resolved CARS spectroscopy.[7-10] To

adapt the time-resolved CARS technique for transient and turbulent flow environments, time-to-frequency mapping of the Raman coherence dephasing by a linearly chirped probe pulse was proposed and demonstrated.[11] The capabilities of this method have been revisited recently, and gas-phase thermometry at data-acquisition rates as high as 1 kHz have been achieved.[12] Despite significant performance improvements, the search for experimental implementations that will make this approach more practical still continues.

The approach described here originates from single-beam CARS methods,[13-15] which have several advantages for applications to gas-phase thermometry. First, the single-beam method does not require that multiple beams crossing at a particular point in space. This is particularly important for turbulent flows because the CARS beams may be steered independently as a consequence of the refractive index gradients created in the turbulent combusting medium. Second, because of the large pump/Stokes bandwidth, several Raman modes are excited impulsively through the combination of numerous frequency pairs within the pulse. Third, data-acquisition rates of 1 kHz allow for observation of transient phenomena that occur in reacting flows.

In our method we obtain a temperature measurement by taking advantage of the temperature-dependent decay rate of the CARS signal; however, we do not scan the probe-pulse delay, but instead use three sub-pulses with specific time delays and wavelengths. In order to generate the discrete time-delayed probe pulses, the probe portion of the laser spectrum is shaped by a static phase–amplitude mask. The CARS response is measured in the frequency domain to yield three points on the decay curve. The relative intensities of the measured CARS signals are temperature dependent, and this dependence is obtained through empirical calibration in a temperate-controlled gas oven. As each laser pulse results in the mapping of the coherence dephasing onto the CARS spectrum, single-shot data acquisition is possible, overcoming the need for the time-consuming task of obtaining data as a function of time delay. In a sense, the present work is an alternative to the use of a linearly chirped probe pulse.[11] This digitized time-to-frequency mapping of coherence dephasing is expected to streamline gas-

temperature retrieval, with no need for complex model equations, especially when prior empirical temperature calibration is performed.

Experimental Methods

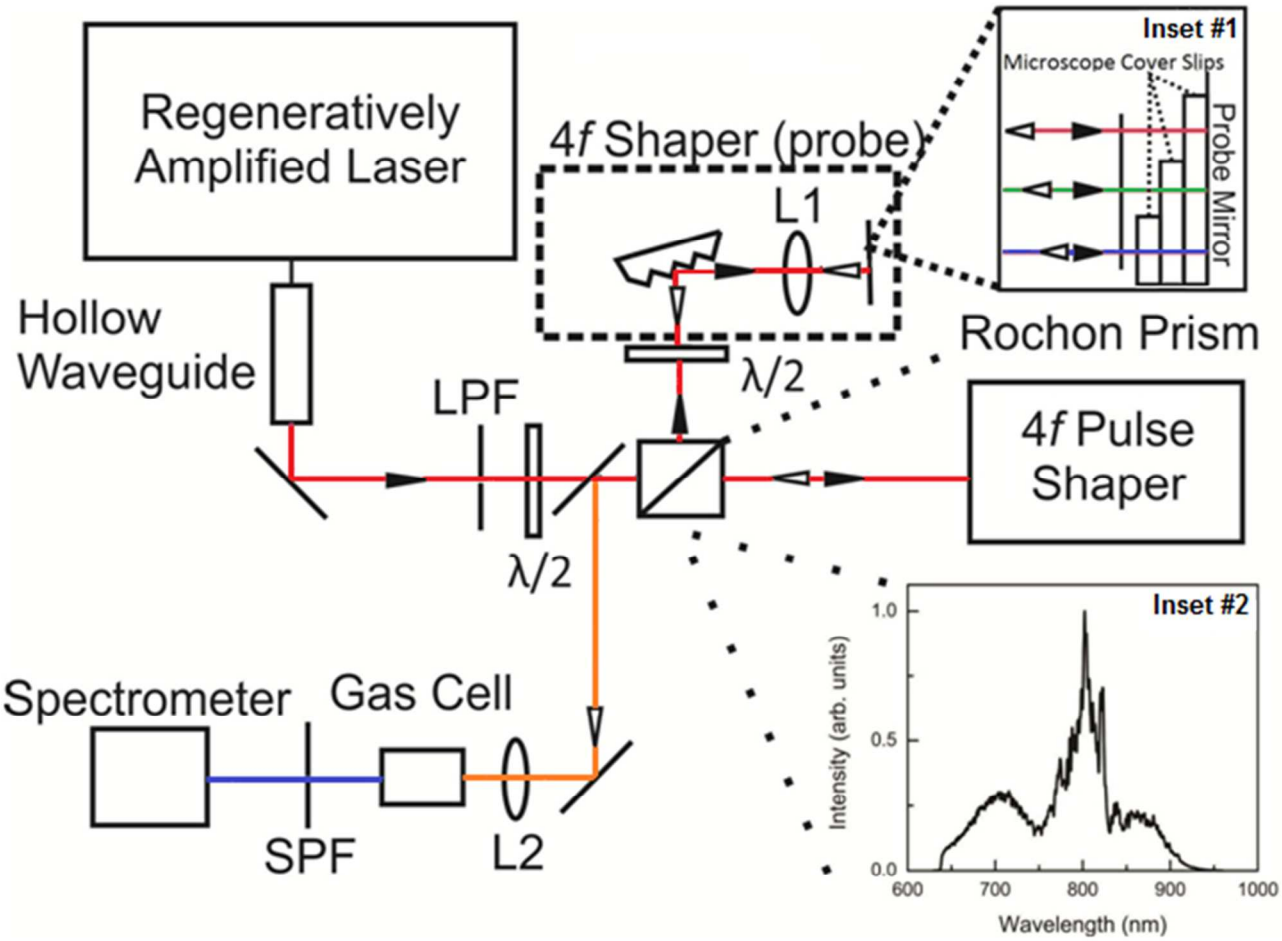

Figure 1. Experimental setup explicitly showing the shaping of the pump and probe portions of the spectrum, which are separated by a polarizing beam splitter (Rochon Prism). LPF, long-pass filter; SPF, short-pass filter; L1–2, lenses. Inset #1: microscope-slide assembly at the Fourier plane of the *4f* shaper used for the probe pulse. Inset #2: Supercontinuum spectrum at the HWG output. The blue side of the spectrum is cut by the 640-nm LPF installed right after the HWG.

Details of the laser used for this work have been published previously.[16] The schematic layout for the experiment is given in Fig. 1. Briefly, a laser supercontinuum that extends from 600–950 nm (bottom-

to-bottom) was produced by self-phase modulation in the hollow waveguide (HWG), a 39-cm long glass capillary filled with argon at approximately 2 bar. The HWG was pumped by the 800-nm output of a 1-kHz Ti:sapphire regenerative amplifier (Legend, Coherent Inc.), seeded by a Micra oscillator (Coherent Inc.). A pulse shaper (FemtoFit, Biophotonic Solutions Inc.), installed between the oscillator and amplifier (not shown), was used to correct high-order phase distortions of pulses at the amplifier output. The linear chirp was then tuned to optimize the supercontinuum bandwidth. The HWG supercontinuum was cut by a 640-nm long-pass filter (see spectrum in Inset #2 in Fig. 1). The beam polarization was tuned by a half-waveplate that effectively split the input intensity at a Rochon prism between the probe and pump/Stokes arms.

In the pump/Stokes arm, a home-built folded-4*f* pulse shaper with a dual-mask 640-pixel spatial light modulator (CRi SLM-640-D) was used. Transform-limited pulses were obtained at the sample by carrying out multiphoton intrapulse interference phase scan (MIIPS).[17,18] After dispersion compensation, the full-width-at-half-maximum (FWHM) pulse duration was approximately 7 fs.

The probe arm featured an optical delay line and a static folded-*4f* shaper. To generate the multiple probes, three microscope cover slips were glued together in a stepwise fashion and attached to a silver-coated mirror at the Fourier plane of the shaper; see Inset #1 in Fig. 1. A static black-foil grid mask was placed on top of the microscope-slide assembly to introduce spectral gaps between those three bands. The different glass thickness for each probing region resulted in ~0.5-ps delay between adjacent bands, thus generating CARS signals at different points in time, as illustrated in Fig. 2.

After shaping both pump and probe beams, the two spectral portions were recombined by the same Rochon prism used to separate them, and were then focused by a 150-mm focal length achromatic lens into a custom-built temperature-controlled gas cell. The average powers in the pump/Stokes and probe beams right before the cell were 8.6 mW and 21 mW, respectively. The generated CARS signal was isolated from the pump/Stokes and probe photons by a 650-nm shortpass filter and detected using a 0.27-m spectrometer with a back-illuminated CCD (PIXIS100, Princeton Instruments).

Results and Discussion

Measurements were performed in the gas cell filled with air. While the CARS signal from both N_2 and O_2 Raman transitions was observed, only the signal from N_2 was analyzed. The gas cell was vacuum-pumped down to 0.52 bar at room temperature and then sealed to preserve the number density throughout heating.

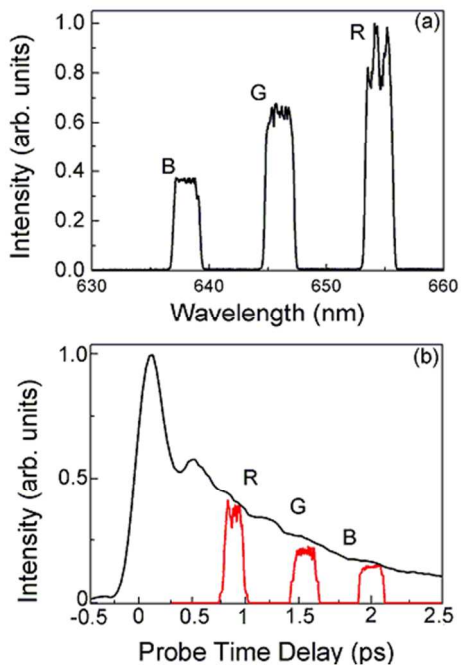

Figure 2. Time-to-frequency mapping by multi-pulse probing: (a) Probe spectrum showing three distinct bands, denoted as R, G, and B. Each of these bands corresponds to different time delays provided by glass slides as shown in the Fig. 1 insert; (b) The single-shot CARS spectrum acquired using the multiple-probe (red line) is overlaid with the time-resolved CARS trace (black line) for the 2330 cm^{-1} Raman transition of N_2 at room temperature.

Our implementation of the time-to-frequency mapping is illustrated in Fig. 2. We selected three frequency gates in the probe beam, as shown in Fig. 2a, and designated them as R, G, and B. These correspond to three regions where the probe delay changes due to the increasing thickness of glass, as shown in the Fig. 1 insert. The time of arrival for each of the probe pulses can be obtained by cross-correlating the pulses with the pump/Stokes beam in the gas cell (data not shown). In Fig. 2b we show a measured CARS transient decay and the corresponding multi-probe single-shot spectrum mapped into

the time domain with the three probe pulses. Note that the single-shot spectrum (red line) is obtained in the frequency domain; therefore, in a single laser shot we obtain the relative intensity at three different points in time. Minor discrepancies due to precise timing for each probe pulse and variations in their relative intensities because of bandwidth or other experimental imperfections are corrected during the temperature calibration procedure described next. The temperature calibration was performed by recording CARS spectra for several pre-set temperatures. For each temperature, ten spectra were acquired and divided equally into two groups, calibration and evaluation. Each spectrum was acquired with 20-ms integration time (20 laser pulses). The coherence-dephasing data were background-subtracted, normalized, averaged, intensity-corrected, and then fit to a three-parameter exponential function ($I=Ae^{-Dt}+C$, where parameter D is the empirical dephasing rate). The retrieved data and corresponding fit curves are summarized in Fig. 3. The dephasing rate changes monotonically with the gas temperature. The dependence is well fit by a linear function (with a coefficient of determination R^2 of 0.995; see Fig. 4).

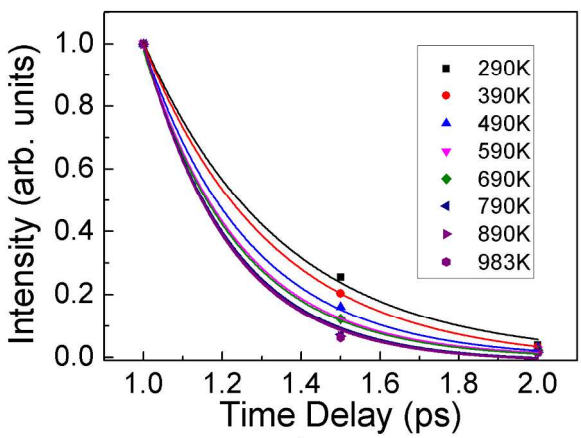

Figure 3. Coherence dephasing of the 2330-cm^{-1} CARS signal from N_2 molecules mapped onto the CARS spectrum by multi-color probing for different gas temperatures. The intensity-corrected peaks are fit by a three-parameter exponential function.

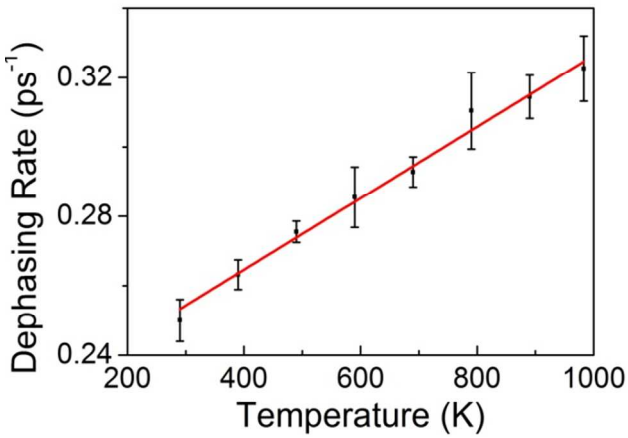

Figure 4. Temperature calibration: retrieved coherence-dephasing rates plotted as a function of gas temperature and fit with a linear function.

In order to confirm that the dephasing rate was not dependent on either the number density/pressure in the focal volume or the laser power, two studies were performed with varying number density/pressure and laser power. These studies (see Supporting Information) demonstrated no dependence on either factor.

To evaluate the accuracy and precision of the temperature calibration, we analyzed gas-temperature measurements from calibration CARS spectra before averaging. Following the same procedure, the intensity-corrected peaks were fit to an exponential function, and dephasing rates were extracted. Those values were then used to create a set of measured temperatures. A comparison between the set (confirmed by thermocouple measurement) and measured temperatures using evaluation spectra is shown in Fig. 5 and demonstrates high accuracy. The difference between the set and measured temperatures remains less than 15 K over the whole range. The measurement precision remains relatively constant, as indicated by the size of the error bars in Fig. 5.

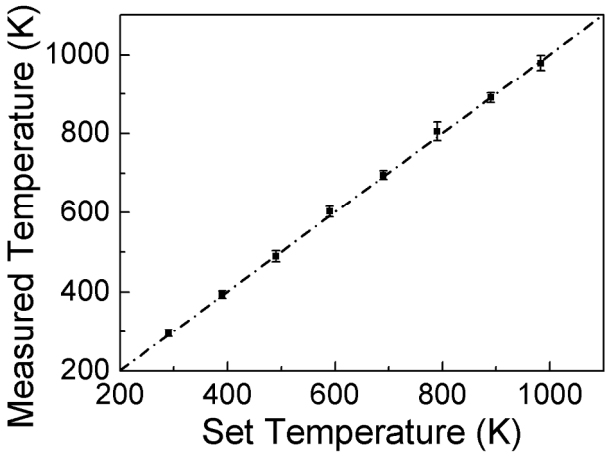

Figure 5. Gas-phase thermometry: measured gas temperature based on calibrated multi-pulse time-to-frequency mapping of coherence dephasing vs. set temperature in the cell.

In order to evaluate the potential of the temperature calibration as a single-shot method, we performed single-shot measurements at 290 K and 433 K. Using the calibration determined in Fig. 4, we converted the single-shot spectra into temperature-measurement data shown in Fig. 6. The accuracy of the measurement remains within ±25 K and ±40 K for 290 K and 433 K, respectively. This demonstrates accurate gas-phase temperature measurement on a picosecond time scale, only accessible with a single-shot technique. However, a more efficient signal generation and collection will be needed for higher temperatures.

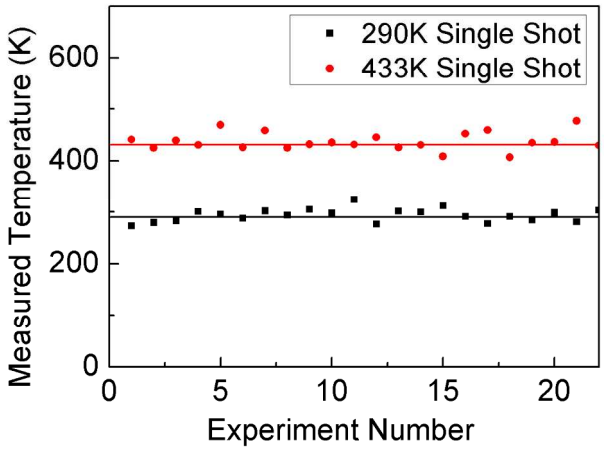

Figure 6. Single-shot thermometry: measured gas temperatures; note black and red line denote set temperature at 290 K and 433 K, respectively. Measured temperatures were 294±25 K and 438±40 K.

Conclusions

We have demonstrated a simple and effective technique for gas-phase thermometry via single-beam, femtosecond CARS spectroscopy. In our approach, the dependence of coherence dephasing on the local gas temperature is mapped into the frequency domain by a short sequence of probe pulses and is fit to an exponential function. The extracted dephasing rate is related to the gas temperature through empirical pre-calibration and is shown to determine the gas temperature with accuracy better than 15 K. Single-shot thermometry measurements are also demonstrated. In principle, the technique allows for single-shot temperature measurements for multiple species, as more than one Raman transition can be monitored at the same time with appropriate spectral probe spacing to avoid interference. Higher pulse energies and tighter focusing can significantly improve the signal-to-noise ratio and the measurement accuracy and precision, especially at high temperatures (low gas densities) such as those in a flame. The timing and the number of colored probe pulses can also be optimized for a particular temperature range.

Acknowledgment. Funding for this research was provided by the Air Force Research Laboratory under Contract No. FA8650-10-C-2008 and by the Air Force Office of Scientific Research (Dr. Enrique Parra, Program Manager).

Supporting Information.

1. Experimental evaluation of temperature calibration as a function of density. We find that temperature determination is insensitive to number density.
2. Experimental evaluation of accuracy and precision of temperature evaluation as a function of fluctuations in laser power. We find that the temperature determination is independent of laser power except for very low powers (a factor of four lower than ideal) where precision suffers.
3. Experimental data obtained simultaneously from multiple species. We demonstrate simultaneous acquisition of time decay data obtained for oxygen and nitrogen. We can control the spectral shift and the delay time for each of the probe lines in order to avoid or minimize spectral overlap among the different species being probed.

This information is available free of charge via the Internet at

http://pubs.acs.org

References and Notes

1 A. Materny, T. Chen, M. Schmitt, T. Siebert, A. Vierheilig, V. Engel, and W. Kiefer, Applied Physics B **71** (3), 299 (2000).

2 T. Lang, K. L. Kompa, and M. Motzkus, Chemical Physics Letters **310** (1–2), 65 (1999).

3 P. Beaud, H. M. Frey, T. Lang, and M. Motzkus, Chemical Physics Letters **344** (3–4), 407 (2001).

4 I. Pastirk, V. V. Lozovoy, and M. Dantus, Chemical Physics Letters **333** (1–2), 76 (2001).

5 A. C. Eckbreth, *Laser diagnostics for combustion temperature and species*. (CRC Press, 1996).

6 R. P. Lucht, S. Roy, T. R. Meyer, and J. R. Gord, Applied Physics Letters **89** (25), 251112 (2006).

7 B. D. Prince, A. Chakraborty, B. M. Prince, and H. U. Stauffer, Journal of Chemical Physics **125** (4), 044502 (2006).

8 D. Pestov, R. K. Murawski, G. O. Ariunbold, X. Wang, M. C. Zhi, A. V. Sokolov, V. A. Sautenkov, Y. V. Rostovtsev, A. Dogariu, Y. Huang, and M. O. Scully, Science **316** (5822), 265 (2007).

9 J. D. Miller, M. N. Slipchenko, and T. R. Meyer, Optics Express **19** (14), 13326 (2011).

10 J. D. Miller, S. Roy, M. N. Slipchenko, J. R. Gord, and T. R. Meyer, Optics Express **19** (16), 15627 (2011).

11 T. Lang and M. Motzkus, Journal of the Optical Society of America B **19** (2), 340 (2002).

12 S. Roy, W. D. Kulatilaka, D. R. Richardson, R. P. Lucht, and J. R. Gord, Optics Letters **34** (24), 3857 (2009).

13 D. Oron, N. Dudovich, and Y. Silberberg, Physical Review Letters **90** (21), 213902 (2003).

14 H. W. Li, D. A. Harris, B. Xu, P. J. Wrzesinski, V. V. Lozovoy, and M. Dantus, Applied Optics **48** (4), B17-B22 (2009).

15 S. Roy, P. Wrzesinski, D. Pestov, T. Gunaratne, M. Dantus, and J. R. Gord, Applied Physics Letters **95** (7), 074102 (2009).

16 M. T. Bremer, P. J. Wrzesinski, N. Butcher, V. V. Lozovoy, and M. Dantus, Applied Physics Letters **99** (10), 101109 (2011).

17 V. V. Lozovoy, I. Pastirk, and M. Dantus, Optics Letters **29** (7), 775 (2004).

18 B. W. Xu, J. M. Gunn, J. M. Dela Cruz, V. V. Lozovoy, and M. Dantus, J. Opt. Soc. Am. B **23** (4), 750 (2006).

Table of Contents Image